Research on Chemical Intermediates
https://doi.org/10.1007/s11164-019-04042-5

Synthesis of a novel hyperbranched polymer and its application in multi-channel sensing Fe^{3+}

Tengxuan Tang[1] · Jing Wang[1] · Dongmei Xu[1]

Received: 14 August 2019 / Accepted: 6 November 2019

Abstract

A novel hyperbranched polymer was designed and synthesized as a spectral probe for Fe^{3+}. The polymer showed high selectivity and sensitivity to Fe^{3+} in CH_3CN/H_2O (75/25, v/v). Fe^{3+} caused a new peak at 560 nm in UV–Vis absorption, a 31 nm fluorescence redshift, a 35-fold enhancement in fluorescence intensity at 575 nm and an 8.3-fold enhancement in fluorescence quantum yield, accompanied by a visual color change from colorless to pink and a fluorescence from dark to bright orange. The colorimetric and fluorescent detection limits were 1.29 and 1.88 μM, respectively. The detection was almost not interfered by other common metal cations. The polymer could be applied in assaying Fe^{3+} in real sample with similar precision to that of atomic absorption spectroscopy.

Keywords Hyperbranched polymer · Rhodamine · Probe · Fe^{3+}

Introduction

Trivalent iron (Fe^{3+}) plays a vital role in the environment and organisms. Its deficiency or overload will cause diseases like anemia, liver dysfunction, diabetes, hemochromatosis and cancer [1–3]. Therefore, the monitoring of Fe^{3+} in environment and organisms is of great importance. In recent years, spectral probe has received much attention in the detection of environmental and biological Fe^{3+} because of its rapid response, high sensitivity, specificity, low-cost and real-time monitoring [4–13].

Electronic supplementary material The online version of this article (https://doi.org/10.1007/s11164-019-04042-5) contains supplementary material, which is available to authorized users.

✉ Dongmei Xu
xdm.sd@163.com

[1] College of Chemistry, Chemical Engineering and Materials Science, Soochow University, Suzhou 215123, Jiangsu, China

Published online: 13 November 2019

Most turn-on spectral probes for Fe^{3+} were based on the rhodamine scaffold [14–21]. However, the reported small molecule probes had some problems such as poor selectivity and easy to lose. Recently, some researchers devoted into studying macromolecular fluorescence probe to overcome the inadequacy [22, 23] because the microenvironment of the polymer chains is in favor of improving the probe's selectivity and the macromolecular backbone of the polymer can resist the probe's loss.

Reversible addition–fragmentation chain transfer (RAFT) polymerization has been considered as one of the most practical polymerization methods for controlling the molecular weight and distribution. Moreover, RAFT polymerization can be carried out by one-pot reaction and relatively easily generate hyperbranched polymer with multiple terminal groups which benefits further modification [24–27].

In this work, we designed and synthesized a hyperbranched polymeric spectral probe by using a rhodamine derivative to modify the epoxy groups in a RAFT polymer. The probe showed excellent sensitivity and selectivity to Fe^{3+} through multiple channels.

Experimental

Synthesis of PGMN2

The reagents and instruments could be found in Supplementary material. Hyperbranched polymeric spectral probe PGMN2 was synthesized by the reaction between the small molecular rhodamine derivative (RE1N2) and the RAFT polymer PGM as illustrated in Scheme 1.

The rhodamine derivative (RE1N2) and the inimer (MCP) were synthesized according to the references [25, 28]. To a stirred solution of rhodamine B (0.5 g, 1.13 mmol) in ethanol (15 mL), ethylenediamine (0.5 mL, 7.5 mmol) was added and the mixture was refluxed overnight under N_2 protection. After cooled to the room temperature, the solvent was removed under reduced pressure and then the residue was dissolved in 20 mL dichloromethane (DCM). The organic solution was washed with water twice, and DCM was removed by evaporation. Earthy yellow solid RE1N2 (0.4703 g, yield 86.3%) was obtained after dried in vacuo. To a stirred solution of 4-cyanopentanoic acid dithiobenzoate (4-CPDB) (0.5 g, 1.79 mmol) in dry DCM (25 mL), hydroxyethyl methylacrylate (HEMA) (235 μL, 1.93 mmol) and 4-dimethylamino pyridine (DMAP) (0.045 g, 0.37 mmol) were added and then *N*,*N*′-Dicyclohexylcarbodiimide (DCC) (1 g, 4.86 mmol) was dissolved in 50 mL dry DCM and dropped into the solution. The mixture was reacted in the ice-water bath for 24 h under N_2 protection. The crude product was obtained by filtration, water-washing and Na_2SO_4-drying. The crude product was further purified through silica gel chromatography with petroleum ether/ethyl acetate (10/1, v/v) as eluent. MCP was gotten as a pink liquid (0.5726 g, yield 69.2%). The ^{1}H NMR spectra of RE1N2 (Fig. S1) and MCP (Fig. S2) were in line with the references.

The RAFT polymer PGM was synthesized in a similar way to the literature [26]: MCP (0.2 g, 0.5 mmol) was dissolved in 10 mL dioxane and dropped into a

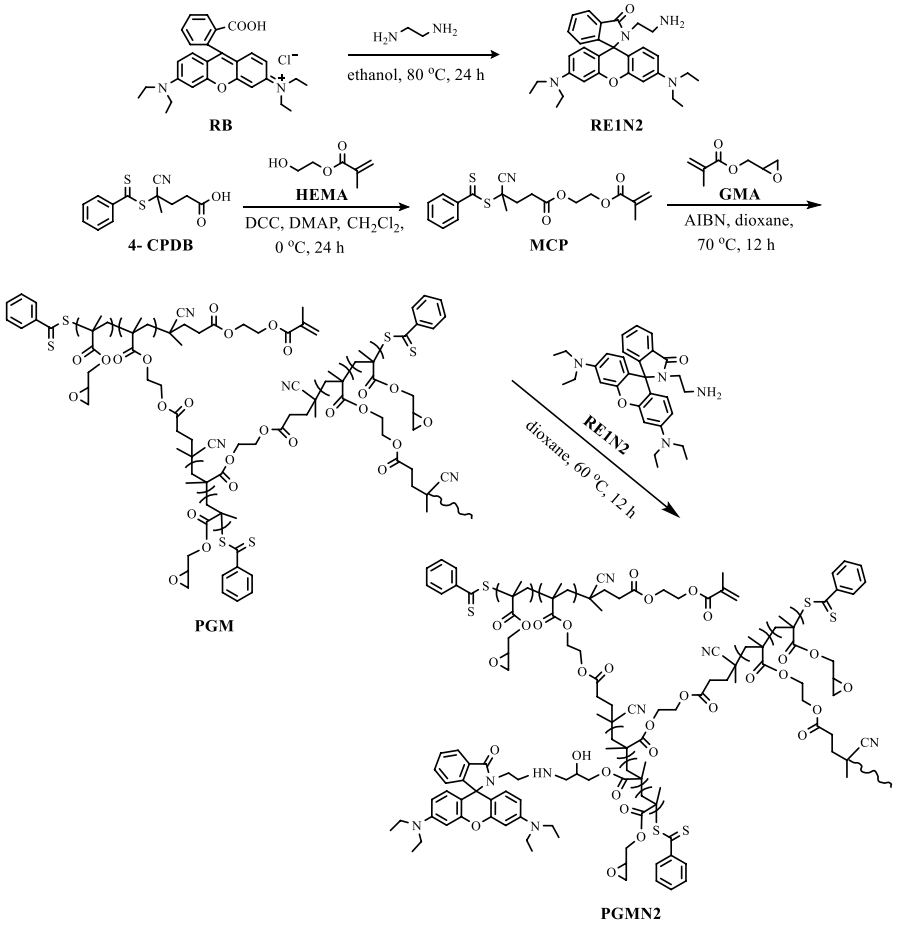

Scheme 1 Synthetic route of PGMN2

100 mL round flask, and then glycidyl methacrylate (GMA) (1.3 mL, 10 mmol) and 2,2′-azobis(isobutyronitrile) (AIBN) (16 mg, 0.1 mmol) were added. The mixture was reacted at 70 °C for 12 h under N_2 protection. After precipitation in cold methanol and dried in vacuum, 0.8792 g (54.2% total monomer conversion) PGM was gotten. Its number average molecular weight (Mn) was 10,200 and the polydispersity (PDI) was 1.71 (Fig. S3). ^{1}H NMR (400 MHz, $CDCl_3$, δ/ppm): 0.93 (s, C(CH_3)COO and C(CN)(CH_3) from MCP), 1.09 (s, C(CH_3)COO from GMA), 1.18–1.26 (m, C(CH_3)(COO)CH_2 and C(CN)(CH_3)CH_2 from MCP), 1.50 (s, CH_2=CCH_3 from MCP), 1.86–1.92 (t, J = 7.2 Hz, C(CN)(CH_3)CH_2CH_2COO from MCP), 1.97 (s, C(CH_3)(COO)CH_2 from GMA), 2.64 and 2.85 (s, CH_2O from GMA), 3.24 (m, CH from GMA), 3.69–3.73 (t, J = 6.8 Hz, COOCH_2CH_2OCO from MCP), 3.80 and 4.31 (s, COOCH_2 from GMA), 5.64 and 6.20 (s,

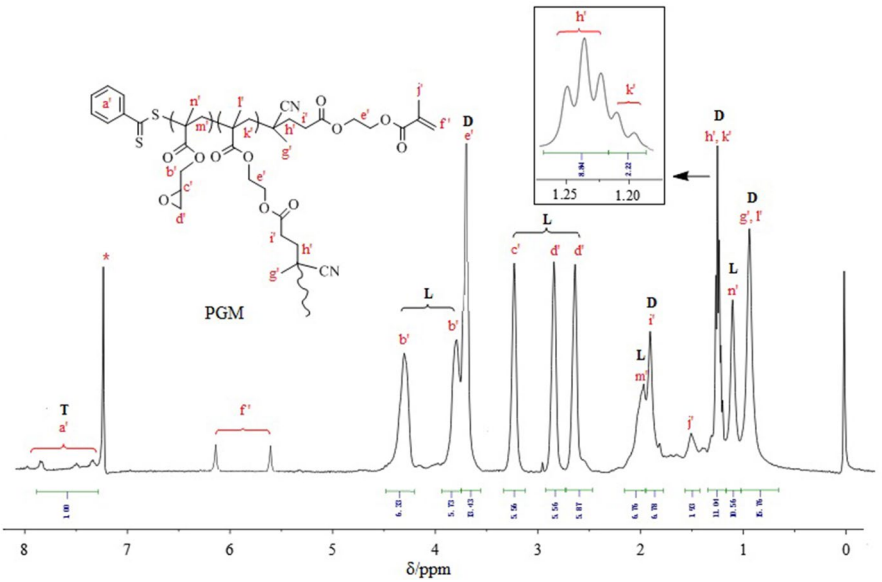

Fig. 1 ^{1}H NMR spectrum of PGM ($CDCl_3$, 400 MHz)

C=CH_2), 7.40–7.91 (m, Ar*H*) (Fig. 1). FT-IR: 3001 (Ar), 2937, 2885 (CH_3, CH_2), 1723 (C=O), 1484, 1452, 1393 (Ar), 1258, 1148 (C–O–C), 907 (epoxy) (Fig. S4).

PGM (0.2 g) was dissolved in 12 mL dioxane in a 100 mL round flask, and RE1N2 (0.03 g, 0.06 mmol) was added. The mixture was protected by N_2 and reacted at 60 °C for 8 h, then precipitated in 20 mL cold methanol, washed with cold methanol (10 mL × 3) to remove unreacted RE1N2 and dried in vacuum, and 0.195 g (yield 85.0%) faint yellow solid PGMN2 was achieved. The number average molecular weight and polydispersity of PGMN2 were 12,200 and 1.92 (Fig. S3). ^{1}H NMR (400 MHz, $CDCl_3$, δ/ppm): 0.93–1.98 (m, CH_3 and CH_2 except those specified below), 2.64 and 2.84 (s, CH_2O from GMA, NHCH_2CH(OH) from the reaction of PGM and RE1N2), 3.24 (s, C*H* from GMA, NHCH$_2$C*H*(OH) from the reaction of PGM and RE1N2), 3.31–3.35 (m, NCH_2CH_2NH from RE1N2), 3.52–3.56 (t, J = 6.8 Hz, COOCH_2CH_2OCO from MCP), 3.80 and 4.31 (s, COOCH_2 from GMA, COOCH_2CH(OH) from the reaction of PGM and RE1N2), 5.64 and 6.01 (s, C=CH_2), 6.24–6.48, 7.10 (m, Ar*H* from RE1N2), 7.40–7.91 (m, Ar*H* from PGM and RE1N2) (Fig. 2). FT-IR: 3440 (OH, NH), 3064 (Ar), 2967, 2851 (CH_3, CH_2), 1728(C=O, ester), 1618 (C=O, amide), 1548, 1489, 1451,1398 (Ar), 1264, 1163 (C–O–C), 1121 (C–N), 908 (epoxy) (Fig. S4).

Spectra study of PGMN2

PGMN2 was dissolved in 10 mL CH_3CN to get a 5 mg/mL stock solution. Metal salts were dissolved in deionized water to get 1.0×10^{-2} mol/L stock solutions.

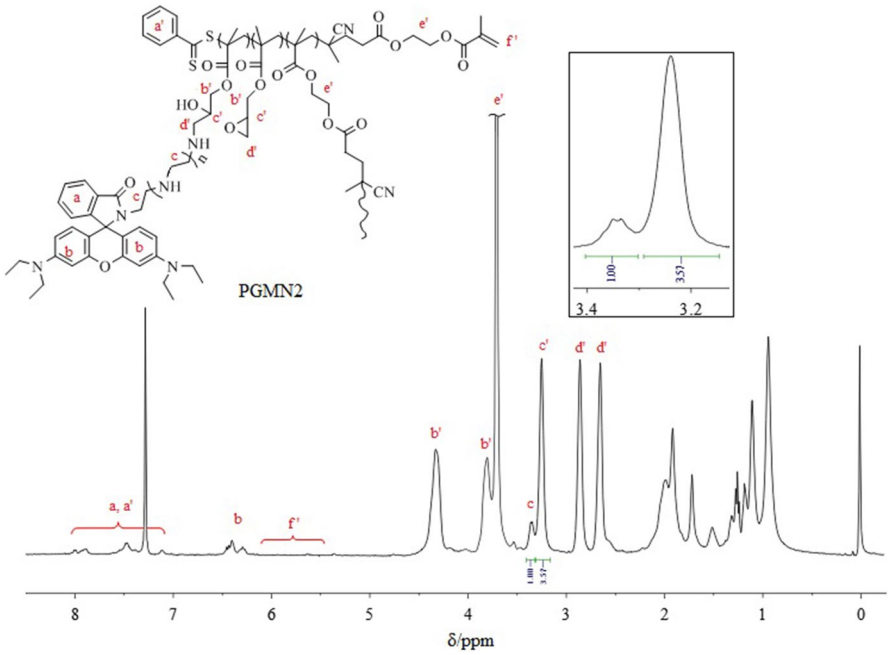

Fig. 2 ^{1}H NMR spectrum of PGMN2 ($CDCl_3$, 400 MHz)

When studying the selectivity of PGMN2 to metal ions, 100 μL stock solution of PGMN2 and one of the metal ion stock solutions were added to a 10 mL volumetric flask. To demonstrate the anti-interference of other metals, one of the metal ion stock solutions except Fe^{3+} (250 μL) was individually added to a 10 mL volumetric flask containing PGMN2 (100 μL) and Fe^{3+} (250 μL). In the fluorescence titration experiment, 100 μL PGMN2 solution was mixed with a certain amount of Fe^{3+} stock solution. All samples were diluted to volume with CH_3CN and H_2O. The medium for the UV–Vis absorption and fluorescence spectra measurement was CH_3CN/H_2O (75/25, v/v). The pH was adjusted by 0.1 mol/L HCl and 0.1 mol/L NaOH aqueous solutions.

Detecting Fe^{3+} in real sample

1 mL pond water (after filtration) or tap water from Dushu Lake Campus of Soochow University was added into a 10 mL volumetric flask, and then PGMN2 (100 μL) and Fe^{3+} stock solutions (100 or 180 μL) were added. PGMN2 method: The mixture was eventually diluted to volume with CH_3CN and H_2O, and the fluorescence spectra were recorded. The concentration of Fe^{3+} in the samples was obtained from the linear relationship between the maximal fluorescence intensity of the sample and the Fe^{3+} concentration. AAS method: The mixture was diluted to volume

with 0.1 mol/L HCl, and the Fe^{3+} concentration in the samples was determined by an AA240FS-GTA120 atomic absorption spectrometer.

Results and discussion

Structure parameters of the hyperbranched PGM and PGMN2

The hyperbranched polymer PGM was generated by RAFT copolymerization of GMA and the intermediate MCP which was from 4-CPDB esterified with HEMA.

In the ^{1}H NMR spectrum of PGM (Fig. 1), the integrals (I) of the peaks representing the linear element (L), branching element (D) and terminal element (T) were $I_L = I_{b'} + I_{c'} + I_{d'} + I_{m'} + I_{n'} = (6.33 + 5.73) + 5.56 + (5.56 + 5.87) + 6.76 + 10.56 = 46.37$, $I_D = I_{e'} + I_{i'} + (I_{h'} + I_{k'}) + (I_{g'} + I_{l'}) = 13.43 + 6.78 + (6.47 + 4.52) + 15.75 = 46.95$ and $I_T = I_{a'} = 1.00$. Based on the Ref. [29], the degree of branching (DB) $= (I_D + I_T)/(I_D + I_T + I_L) \approx 0.50$.

From ^{1}H NMR spectrum (Fig. 1) and GPC (Fig. S3) of PGM, the signal at 7.87 was from the phenyl of MCP and the peak at 3.24 was from the epoxy group of PGM. The number average chain transfer agent functionality (Fn) in per hyperbranched PGM was 1.71 based on the equation $Fn = Mn_{PGM} \times I_{7.87}/(Mw_{MCP} \times I_{7.87} + 2Mw_{GMA} \times I_{3.24})$, in which M_{WMCP} and M_{WGMA} were molecular weight of MCP and GMA. By comparing the integration of the peaks at 7.87 ($I_{7.87}$) and 3.24 ($I_{3.24}$) ppm, the molar ratio (R) of GMA to MCP was determined to be 39.52 ($R = 2I_{3.24}/I_{7.87}$). Hence, each hyperbranched PGM contained about 67.6 (Fn × R) GMA units [26].

The spectral probe PGMN2 was synthesized through PGM functionalized with rhodamine unit RE1N2. The number of RE1N2 in PGMN2 based on GPC was calculated by the number average molecular weight (Mn) of PGMN2 and PGM as well as the molecular weight of RE1N2 according to the equation $m = [Mn_{PGMN2} - Mn_{PGM}]/M_{RE1N2}$. The result was 4.12. Alternatively, in the ^{1}H NMR spectrum of PGMN2 (Fig. 2), the chemical shift at 3.35 was the signal of hydrogen in the ethanediamine of rhodamine unit and the chemical shift at 3.24 was belonged to the epoxy unit of PGM. According to the integral (I) of these two peaks, 6.54% [$I_{3.35}/(I_{3.35} + 4I_{3.24})$] of GMA units was estimated to take part in the epoxy ring opening reaction. Therefore, the number of RE1N2 grafted to PGM was 4.42 (6.54% × 67.6) [26] which was near to 4.12 from GPC.

Selectivity and sensitivity of PGMN2 to Fe^{3+}

Solubility of PGMN2 was studied, and it was found that PGMN2 was poorly dissolved in methanol, ethanol and deionized water (H_2O), moderately dissolved in CH_3CN and DMF, and well dissolved in solvents with medium polarity such as DCM, THF, acetone and dioxane. Both solubility, practicality and environment amity are considered, the mixture of CH_3CN and H_2O was selected as the sensing medium.

The selectivity of hyperbranched spectral probe PGMN2 to common metal ions such as Ca^{2+}, Mg^{2+}, K^{+}, Na^{+}, Fe^{2+}, Cu^{2+}, Fe^{3+}, Zn^{2+}, Co^{2+}, Mn^{2+}, Pb^{2+}, Ni^{2+}, Cr^{3+}, Cd^{2+}, Hg^{2+} and Ag^{+} was investigated by UV–Vis absorption and fluorescence spectroscopy in CH_3CN/H_2O (75/25, v/v). As shown in Fig. 3, only when Fe^{3+} was added into the PGMN2 solution, an apparent peak at 565 nm accompanied by a naked-eye observed color change from colorless to pink appeared in the UV–Vis absorption spectra (Fig. 3a). Similarly, a 31 nm fluorescence redshift, a 35-fold fluorescence enhancement at 575 nm and an 8.3-fold enhancement in fluorescence quantum yield (using rhodamine B in ethanol as the reference standard, $\Phi = 0.97$) with the emerging of a bright orange fluorescence color after Fe^{3+} were added (Fig. 3b). All these results exhibited that PGMN2 was highly selective and sensitive to Fe^{3+} and had the potential to be utilized as a turn-on highly selective and sensitive multi-channel spectral probe for Fe^{3+}.

UV–Vis absorption and fluorescence titration with Fe^{3+}

In order to investigate the possibility of PGMN2 used as the spectral probe for Fe^{3+}, titration experiment was done and the results are shown in Fig. 4. The absorbance at 565 nm in UV–Vis absorption spectra showed a linearly proportional relationship with the concentration of Fe^{3+} ranging from 40 to 240 μM (Fig. 4a), and the correlation coefficient was 0.993. In addition, the fluorescence intensity at 575 nm had a linear response toward Fe^{3+} with a correlation coefficient of 0.992 (Fig. 4b). The DLs evaluated from colorimetric and fluorescent titrations [19] were 1.29 and 1.88 μM, respectively. The results proved the hypothesis that PGMN2 could quantitatively trace Fe^{3+} in CH_3CN/H_2O (75/25, v/v) by multiple channels.

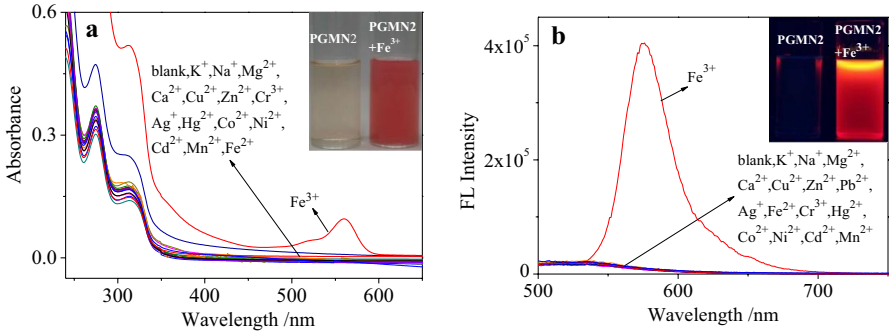

Fig. 3 UV–Vis absorption (**a**) and fluorescence (**b**) spectra of PGMN2 in the absence and presence of various cations. Solvent: CH_3CN/H_2O (75/25, v/v). Concentration: 50 μg/mL for PGMN2, 200 μM for metal ions. λ_{ex}: 467 nm, slit width: 5 nm

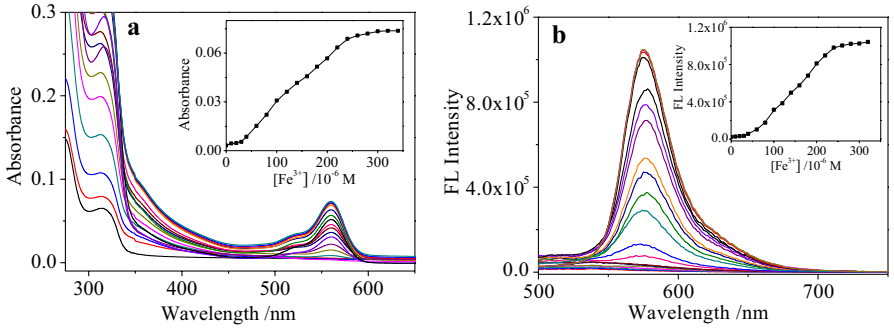

Fig. 4 UV–Vis absorption (**a**) and fluorescence (**b**) spectra of PGMN2 with various concentrations of Fe^{3+}. Solvent: CH_3CN/H_2O (75/25, v/v), concentration: 50 μg/mL for PGMN2, from bottom to top, Fe^{3+}: 0, 10, 20, 30, 40, 60, 80, 100, 120, 140, 160, 180, 200, 220, 240, 260, 280, 300 and 320 μM. Insets: the relationship between the absorbance at 560 nm/fluorescence intensity at 575 nm and the concentration of Fe^{3+}. λ_{ex}: 467 nm, slit width: 5 nm

Effect of coexisting ions

In order to figure out if other common metal cations will influence the detection of Fe^{3+} by PGMN2, K^+, Na^+, Mg^{2+}, Cu^{2+}, Zn^{2+}, Cr^{3+}, Fe^{2+}, Ca^{2+}, Pb^{2+}, Hg^{2+}, Ni^{2+}, Mn^{2+}, Co^{2+}, Cd^{2+} and Ag^+ were introduced into the solution of PGMN2-Fe^{3+} individually, and the absorption and fluorescence spectra were recorded, respectively (Fig. 5). The experiments showed that the addition of these cations had negligible influence on the absorption and fluorescence maxima of PGMN2-Fe^{3+} solution, which indicated the excellent anti-interference performance of PGMN2 for monitoring Fe^{3+}.

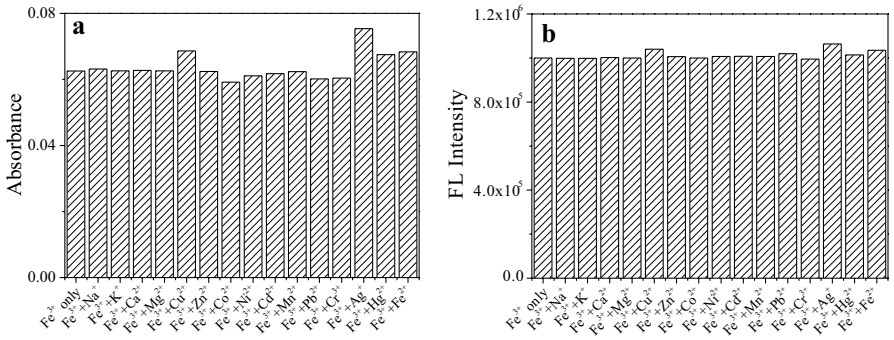

Fig. 5 Effects of coexisting ions on the UV–Vis absorbance at 560 nm (**a**) and fluorescence intensity at 575 nm (**b**) of the PGMN2-Fe^{3+} solutions. Solvent: CH_3CN/H_2O (75/25, v/v). Concentration: 50 μg/mL for PGMN2, 300 μM for ions. λ_{ex}: 467 nm, slit width: 5 nm

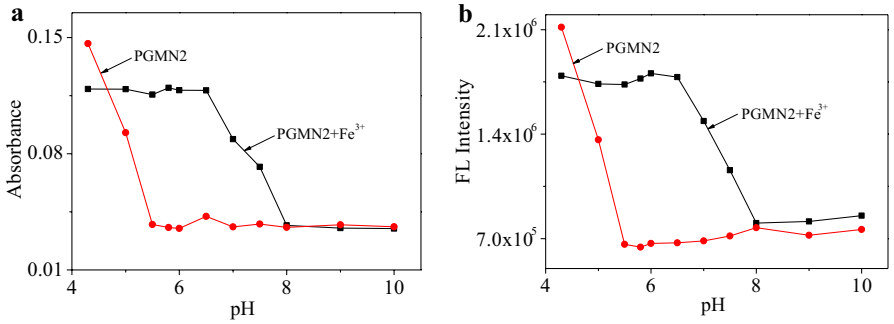

Fig. 6 Effects of pH on the absorbance at 560 nm (**a**) and fluorescence intensity at 575 nm (**b**) of PGMN2 and PGMN2-Fe^{3+}. Solvent: CH_3CN/H_2O (75/25, v/v), concentration: 50 μg/mL for PGMN2, 300 μM for Fe^{3+}, pH: 4.3, 5.0, 5.5, 5.8, 6.0, 6.5, 7.0, 7.5, 8.0, 9.0 and 10.0. λ_{ex}: 467 nm, slit width: 5 nm

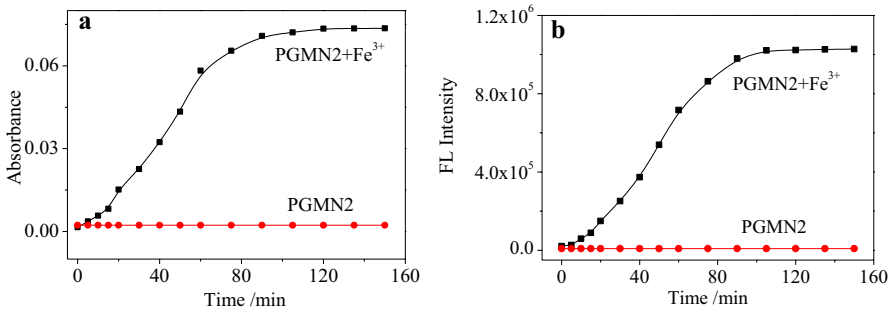

Fig. 7 Kinetics of PGMN2 sensing Fe^{3+} by UV–Vis absorption (**a**) and fluorescence (**b**) spectra. Solvent: CH_3CN/H_2O (75/25, v/v), concentration: 50 μg/mL for PGMN2, 300 μM for Fe^{3+}. λ_{ex}: 467 nm, slit width: 5 nm

Effect of pH

To know the acid and alkali media suitable for PGMN2, the UV–Vis absorption and fluorescence spectra of PGMN2 and PGMN2-Fe^{3+} in the pH range of 4.3–10.0 (Fig. 6) were studied. The absorbance at 560 nm (A_{560}) (Fig. 6a) and the fluorescence intensity at 575 nm (F_{575}) (Fig. 6b) of the solutions before and after introducing Fe^{3+} coincided at pH 4.7 and pH 8.0, respectively. However, when pH increased from 5.0 to 7.5, A_{560} and F_{575} of the PGMN2-Fe^{3+} solutions were obviously larger than those of the PGMN2 solutions with the same pH. Therefore, PGMN2 could be applied to monitor Fe^{3+} in the pH range of 5.0–7.5.

Kinetics of PGMN2 sensing Fe^{3+}

The time dependence of PGMN2 sensing Fe^{3+} by UV–Vis absorption and fluorescence spectra was investigated, and the results are given in Fig. 7. It could be seen

Table 1 Determination of Fe^{3+} in environmental water samples

Method	Sample	Fe^{3+} added (10^{-6} mol/L)	Fe^{3+} found (10^{-6} mol/L)	Recovery (%)	RSD (%)
PGMN2	Tap water	100	102.6	102.6	0.45
		180	178.8	99.3	0.86
	Pool water	100	97.8	97.8	1.46
		180	183.9	102.1	0.73
AAS	Tap water	100	101.1	101.1	1.99
		180	181.3	100.7	1.83
	Pool water	100	99.6	99.6	1.41
		180	180.8	100.4	1.42

Solvent: CH_3CN/H_2O (75/25,v/v), concentration: 50 μg/mL for PGMN2, RSD: Relative standard deviation. Each test was repeated three times

that the reaction between PGMN2 and Fe^{3+} finished almost after 90 min they was mixed.

Real sample assay

We tried to use PGMN2 as a fluorescent probe to determine the amount of Fe^{3+} in spiked tap water and pool water and compared the result with that from AAS (Table 1). The concentration of Fe^{3+} found by PGMN2 and AAS was very closed and both consistent with the Fe^{3+} added. The recovery from PGMN2 was between 97.8% and 102.6% with the relative standard deviation (RSD) of three measurements less than 1.5% which was similar to that from AAS. Therefore, PGMN2 can be applied in the effective detection of Fe^{3+} in environmental water.

Conclusion

In summary, this paper discussed a novel rhodamine-based hyperbranched polymeric turn-on colorimetric and fluorescent probe PGMN2 for Fe^{3+}. With high selectivity and sensitivity to Fe^{3+} over other common cations, PGMN2 can sense Fe^{3+} by six channels including absorbance increase, fluorescence intensity strengthening, fluorescence quantum yield enhancement, fluorescence redshift, visual color change and fluorescence color change. Moreover, the probe can monitor Fe^{3+} in a wide concentration range, with low detection limit under physiological pH. The probe can also be applied in environmental water sample assay, and its accuracy is similar to that of AAS.

Acknowledgements This work was supported by the National Natural Science Foundation of China (21074085), and the Priority Academic Program Development of Jiangsu Higher Education Institutions.

References

1. N. Roy, A. Dutta, P. Mondal, P.C. Paul, T.S. Singh, Sens. Actuators B Chem. **236**, 719 (2016)
2. Y. Yang, C.Y. Gao, D.W. Dong, Sens. Actuators B Chem. **222**, 741 (2016)
3. Z.Q. Li, Y. Zhou, K. Yin, Z. Yu, Y. Li, J. Ren, Dyes Pigments **105**, 7 (2014)
4. S.K. Dwivedi, R.C. Gupta, R. Ali, S.S. Razi, S.K. Hira, P.P. Manna, M. Arvind, J. Photochem. Photobiol. A **358**, 157 (2018)
5. S. Biswas, V. Sharma, P. Kumar, A.L. Koner, Sens. Actuators B Chem. **260**, 460 (2018)
6. C.J. Hua, H. Zheng, K. Zhang, M. Xin, J.R. Gao, Y.J. Li, Tetrahedron **72**, 8365 (2016)
7. N. Lukasik, E. Wagner-Wysiecka, A. Małachowska, Analyst **144**, 3119 (2019)
8. F.Y. Liu, P.P. Tang, R.H. Ding, L.J. Liao, L.S. Wang, M. Wang, J.Y. Wang, Dalton Trans. **46**, 7515 (2017)
9. L.Y. Wang, G.P. Fang, D.R. Cao, Sens. Actuators B Chem. **207**, 849 (2015)
10. S. Warrier, P.S. Kharkar, Spectrochim. Acta A. **188**, 659 (2018)
11. P. Madhu, P. Sivakumar, J. Photoch. Photobio. A **371**, 341 (2019)
12. Ş. Duygu, Y. Halil, H. Zeliha, Res. Chem. Intermed. **42**, 6337 (2016)
13. G. Meiling, X. Puhui, W. Lingyu, M. Xiaohui, G. Fengqi, Res. Chem. Intermed. **41**, 9673 (2015)
14. S. Goswami, S. Das, K. Aich, D. Sarkar, T.K. Mondal, C.K. Quah, H.K. Fun, Dalton Trans. **42**, 15113 (2013)
15. X.F. Bao, J.X. Shi, X.M. Nie, X.L. Wang, L.Y. Zhang, Bioorg. Med. Chem. **22**, 4826 (2014)
16. M.H. Lee, H. Lee, M.J. Chang, H.S. Kim, C. Kang, J.S. Kim, Dyes Pigments **130**, 245 (2016)
17. H.L. Chen, X.F. Bao, Sens. Actuators B Chem. **242**, 921 (2017)
18. R. Bhowmick, A.S.M. Islam, U. Saha, G.S. Kumar, M. Ali, New J. Chem. **42**, 3435 (2018)
19. J. Xue, L.M. Tian, Z.Y. Yang, J. Photoch. Photobio. A. **369**, 77 (2019)
20. A.S. Murugan, N. Vidhyalakshmi, U. Ramesh, J. Annaraj, Sens. Actuators B Chem. **274**, 22 (2018)
21. M. Ozdemir, Y. Zhang, M.L. Guo, Inorg. Chem. Commun. **90**, 73 (2018)
22. Y. Wang, H.Q. Wu, J. Luo, X.Y. Liu, React. Funct. Polym. **72**, 169 (2012)
23. H.P. Diao, L.X. Guo, W. Liu, L.H. Feng, Spectrochim. Acta A. **196**, 274 (2018)
24. J.B. Jiang, X. Xiao, P. Zhao, H. Tian, J. Polym. Sci. Pol. Chem. **48**, 1551 (2010)
25. Z.K. Wei, X.J. Hao, Z.H. Gan, T.C. Hughes, J. Polym. Sci. Pol. Chem. **50**, 2378 (2012)
26. C.X. Li, H.H. Liu, D.D. Tang, Y.L. Zhao, Polym. Chem. **6**, 1474 (2015)
27. S.Q. Chen, H. Chen, H.J. Li, P.Y. Li, W.D. He, Polym. Chem. **7**, 2476 (2016)
28. B. Bag, Org. Biomol. Chem. **9**, 4467 (2011)
29. M. Jikei, M. Kakimoto, Prog. Polym. Sci. **26**, 1233 (2001)